CIMAC CONGRESS 25
ZURICH, MAY 19 – 23, 2025

2025 | 272

CO2 Reduction Benefits through Engine Room Hybridization by Applying ECMS Algorithm

System Integration & Hybridization

Apostolos Karvountzis-Kontakiotis, WinGD

Nikolaos Aletras, Laboratory of Applied Thermodynamics, Aristotle University of Thessaloniki
Nikolaos Kefalas, Laboratory of Applied Thermodynamics, Aristotle University of Thessaloniki
Paraskevas Karadimitriou, Laboratory of Applied Thermodynamics, Aristotle University of Thessaloniki
Leonidas Ntziachristos, Laboratory of Applied Thermodynamics, Aristotle University of Thessaloniki

ABSTRACT

Carbon emissions from human activities play a key role in the major environmental problem of global warming. The maritime transportation sector is a substantial contributor to carbon emissions, therefore authorities around the world take actions and set targets for reducing CO2 emissions in this sector. Specifically, the international maritime organization (IMO) has introduced carbon intensity indicator (CII) with the target to reduce the carbon intensity of the ship fleet above 5000 gross tonnage by 40% by 2030 compared to 2008. One way to reduce CO2 emissions from ships is the hybridization of their engine rooms by adding shaft-generators and batteries. Hybrid configurations are systems with two or more degrees of freedom, they require a supervisory controller, often called energy management system (EMS), that decides how the individual components operate. EMS has a crucial role in the engine room fuel consumption and therefore optimizing its operation would further decrease CO2 emissions. This can be achieved by utilizing optimization-based algorithms such as the equivalent consumption minimization strategy (ECMS). ECMS offers instantaneous optimal solutions and can significantly contribute to CO2 reduction benefits with a low computational cost. Two ship models were built in the MATLAB Simulink environment utilizing the library components in the powertrain blockset to evaluate the hybrid engine room configuration that utilizes ECMS algorithm against a conventional (non-hybrid) one. The performance of the individual components in terms of fuel and power efficiency maps as well as the propeller resistance curve were collected from experimental tests by the Winterthur Gas & Diesel Ltd on test components of the same configuration. The current study examines the potential CO2 benefits offered by an adaptive ECMS on a ship equipped with a 2-stroke main engine hybridized with shaft-generator. Benefits of the proposed powertrain and algorithm are analyzed for different operating conditions, including the phases of port stay, open sea sailing and port approach. Adapting power systems on ships with the proposed one and adopting energy optimization algorithms could result to immediate CO2 reduction of current ships.

1 INTRODUCTION

Human-generated carbon dioxide (CO_2) emissions are widely acknowledged as the primary driver of global warming [1] with ships significantly contributing to these emissions [2,3]. To tackle this issue, the International Maritime Organization (IMO) has implemented indexes such as the Carbon Intensity Indicator (CII), the Energy Efficiency Design Index (EEDI), and the Energy Efficiency Existing Ship Index (EEXI) with the target to reduce the carbon intensity of the ship fleet above 5000 gross tonnage by 40% by 2030 compared to 2008 [4–7].

One potential solution to meet IMO targets is to reduce CO_2 emissions by hybridizing ship propulsion systems [8]. One method for hybridization allows the main engine (ME) to operate more efficiently by storing surplus power in batteries through a shaft generator (SG) [9]. CO_2 reductions can be achieved by optimizing energy management system (EMS) decisions through energy optimization algorithms [10]. Optimization algorithms for hybrid ships typically rely on dynamic programming (DP), model predictive control (MPC), and equivalent consumption minimization strategy (ECMS) [11] approaches. DP offers a globally optimal solution but necessitates a priori knowledge of the power demand profile of the propulsion system and electrical consumers throughout the trip and incurs significant computational costs [12,13]. MPC can generate solutions approaching optimality, while requiring less computational effort than DP [14–16]. However, a forecast of the power demand profile for a time horizon of 10 to 600 seconds is necessary [14–16]. ECMS mitigates computational cost by determining instantaneous optimal solutions, but potentially results in solutions that diverge from the global optimum compared to DP and MPC [17–19]. However, ECMS does not necessitate any a priori or predicted knowledge of the power demand profile.

ECMS has been applied to hybrid ships utilizing either 4-stroke [20,21] or 2-stroke main engines (ME) [22], with the latter exhibiting superior thermal efficiency [22]. Two-stroke ME, with their high efficiency, enable more efficient electric power generation for electrical consumers through power take-off operation (PTO) with a SG, in comparison to power delivery from 4-stroke auxiliary engines [23]. It is therefore valuable to investigate how this concept can be optimized to further reduce fuel oil consumption (FOC) in hybrid propulsion systems featuring a 2-stroke ME, an area that has not yet been thoroughly explored in the literature.

This study investigates the potential fuel savings achievable by using an adaptive ECMS on a ship equipped with a 2-stroke ME and a SG. The study analyzes the benefits of the proposed powertrain and algorithm under various operating conditions, including port stay, open-sea sailing, and port approach. By adapting power systems on existing ships with this hybrid system and employing energy optimization algorithms, immediate CO_2 reductions can be realized. Additionally, this approach should be considered for new ship builds as well for retrofit solutions.

2 METHODOLOGY

2.1 Examined Topologies

Two ship propulsion system models were created in MATLAB Simulink using components from the powertrain blockset library [24,25] to compare a conventional (non-hybrid) engine room configuration (Figure 1a) with a hybrid one (Figure 1b). The conventional configuration (Figure 1a) consists of two energy converters: the ME and the gensets, both considered to use the same fuel oil grade. In this configuration, the ME delivers mechanical power to the propeller for ship propulsion, while gensets produce electrical power for onboard consumers.

In contrast, the hybrid configuration (Figure 1b) incorporates additional components such as a SG, electrical systems (including transformers and inverters), and a battery pack. These components connect the ME to the electrical consumers, allowing it to supply electrical power through the switchboard. The number of gensets remains the same in both configurations due to the manufacturer's choice. However, in the hybrid configuration, the three gensets exceed the auxiliary power demand and could potentially be optimized and reduced. Furthermore, the battery pack enhances load distribution and provides a reliable, uninterrupted power supply [26].

The performance of individual components was simulated using efficiency tabulated data from real-world sea trial tests conducted by Winterthur Gas & Diesel Ltd.

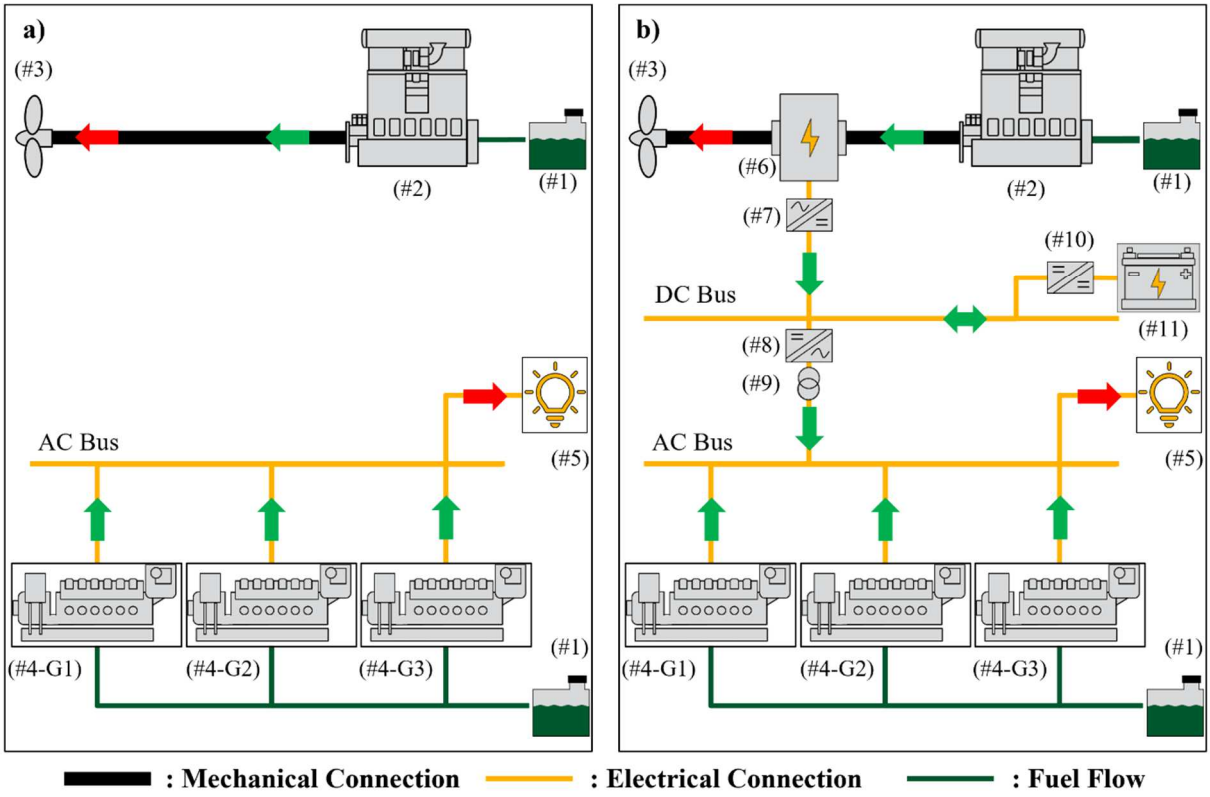

Figure 1. Engine room configurations: conventional (a), hybrid (b), where (#1): fuel tank, (#2): main engine (ME), (#3): propeller, (#4-G1): genset 1, (#4-G2): genset 2, (#4-G3): genset 3, (#5): electrical consumers, (#6): shaft generator (SG), (#7): alternating current (AC) to direct current (DC) converter, (#8): DC to AC converter, (#9): transformer, (#10): DC to DC converter, (#11): battery pack

Table 1. Technical specifications of main components in the engine room configurations

Component	Engine room configuration	
	Conventional	Hybrid
Main engine (ME)	14.78 MW	
Gensets	3 x 1.22 MW	
Shaft-generator (SG)	-	1.30 MW
Battery	-	565 kWh
Propeller type	Fixed pitch propeller	

2.2 Gensets operation rule for the conventional configuration

In the conventional configuration, the gensets are governed by a rather simple rule , as illustrated in Figure 2 [28]. According to this rule, one genset supplies power to the electrical consumers until its load reaches a threshold of 0.85. At this point, a second genset is activated, and the power demand is shared between the two gensets. As the power demand increases, additional gensets are brought in following the same rule (in the case shown in Figure 2, the maximum number of gensets is three). The 0.85 load threshold was chosen to ensure reliable operation and extend the lifespan of the gensets [28].

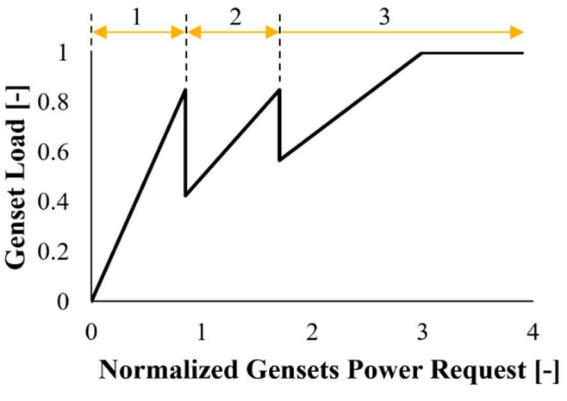

Figure 2. Number of gensets in operation and their operating load according to total normalized power demand

2.3 ECMS implementation for the hybrid configuration

An ECMS algorithm was developed to optimize the performance of the proposed hybrid ship

configuration. Building on previous works [29,30], it was modified and expanded to incorporate the cost factors of the main components in the engine room. This ECMS can also be adapted to account for the performance of significant auxiliary consumers, depending on the specific requirements of the ship. The ECMS cost function ($\dot{m}_{fuel,total}$) is defined in eq. 1, where $\dot{m}_{fuel,total}$ must be minimized with respect to the decision variables u_1 to u_4 (eq. 2– eq. 3).

The ECMS cost function consists of three components for optimization. The first component is the fuel mass flow rate of the main engine ($\dot{m}_{fuel,ME}$), which is dependent on the main engine power. The ME power is a function of the normalized SG load u_1, which ranges from 0 (PTO mode deactivated) to -1 (operation at minimum rated power - $P_{SG,rated}$), as defined by eq. 2, where P_{SG} represents the SG power. The explored range of u_2 is limited to the function of SG operating as a generator ($P_{SG} \leq 0$) for simplicity, excluding its operation as a motor.

The second component is the total fuel mass rate to the gensets ($\dot{m}_{fuel,Gensets}$), which depends on their normalized load functions u_2, u_3, u_4. These range from 0 (genset shut off) to 1 (operation at full power - $P_{Gen,max}$), as outlined in eq. 3, where $P_{Gen,1}$, $P_{Gen,2}$, $P_{Gen,3}$ represent the genset power for the gensets 1 to 3, respectively.

The third component, P_{Batt}, represents the battery's electric power, which can be either positive or negative depending on whether the battery is supplying (discharging) or receiving (charging) electrical energy. An additional cost factor (p) is included in P_{Batt} to maintain the state of charge (SOC) near a target value. P_{Batt} is then converted to an equivalent fuel rate using the equivalence factor (s_{eq}) and the lower heating value (Q_{LHV}) of the fuel oil.

The s_{eq} term is calculated based on eq. 4, which can take two different constant values depending on whether the battery is supplying (s_{dis}) or absorbing (s_{chg}) electrical energy. The p term is parameterized based on eq. 5 provided by Onori et al. [31], which depend on the SOC. Eq. 5 considers a target value for the SOC (SOC_{target}), and selected maximum (SOC_{max}) and minimum (SOC_{min}) values and a superscript for the penalization function (a).

The selected parameters for the calculation of s_{eq} and p are listed in Table 2, based on moderate values by Aletras et al. [30].

$$\dot{m}_{fuel,total}(t) = \dot{m}_{fuel,ME} + \dot{m}_{fuel,Gensets} + \frac{s_{eq}}{Q_{LHV}} \times P_{Batt} \times p(SOC) \quad (1)$$

$$u_1 = \frac{P_{SG}}{P_{SG,rated}} \quad (2)$$

$$\begin{bmatrix} u_2 \\ u_3 \\ u_4 \end{bmatrix} = \begin{bmatrix} \frac{P_{Gen,1}}{P_{Gen,max}} \\ \frac{P_{Gen,2}}{P_{Gen,max}} \\ \frac{P_{Gen,3}}{P_{Gen,max}} \end{bmatrix} \quad (3)$$

$$s_{eq} = \begin{cases} (s_{dis} | P_{Batt} \geq 0) \\ (s_{chg} | P_{Batt} < 0) \end{cases} \quad (4)$$

$$p(SOC) = 1 - \left(\frac{SOC(t) - SOC_{target}}{(SOC_{max} - SOC_{min}) \times 0.5} \right)^a \quad (5)$$

Table 2. ECMS algorithm parameters

Parameter	Value
s_{dis}	3.6
s_{chg}	1.1
a	1
SOC_{target}	0.5
SOC_{max}	0.8
SOC_{min}	0.2

The ECMS optimization adheres to the constraints outlined in eq. 6 through eq. 11. Eq. 6 describes the mechanical power balance in the hybrid ship configuration, stating that the power required at the propeller (P_{Prop}) must equal the combined mechanical power outputs from the main engine (P_{ME}) and the P_{SG}. If the rotational speed of the propeller is known, P_{Prop} can be calculated using the propeller curve. Consequently, eq. 6 can be utilized to determine P_{ME}.

Eq. 7 outlines the electrical power balance in the hybrid ship configuration. The power required by the electrical consumers ($P_{Consumers}$) must equal the combined electrical power supplied by the SG ($P_{SG,\,electric}$), the gensets ($P_{Gen,all}$), and the P_{Batt}. The values of $P_{SG,\,electric}$ and $P_{Gen,all}$ can be calculated using map-based modeling, which accounts for the efficiencies of the SG and gensets. Therefore, if $P_{Consumers}$ is known, eq. 7 can be used to determine P_{Batt}.

Eq. 8 through eq. 11 define the physical constraints of the components. Eq. 8 specifies that the ME cannot operate beyond its maximum power output ($P_{ME,\,max}$). Eq. 9 restricts the SG to operate within its full load curve and the PTO limitation, with bounds defined by $P_{SG,min}$ and $P_{PTO,limit}$, respectively. The $P_{PTO,limit}$ as a function of rotational speed is illustrated in Figure A1 in the Appendix. According to eq. 10, the gensets are limited to 85% of their full load curve, where $P_{Gen,i}$ represents the power of the genset, with i index

denoting the genset number. Lastly, to ensure battery longevity, the battery state of charge (SOC) must remain within a specific range, between a maximum (SOC_{max}) and minimum level (SOC_{min}), as outlined in eq. 11.

$$P_{Prop} = P_{ME} + P_{SG} \quad (6)$$

$$P_{Consumers} = P_{SG,\,electric} + P_{Gen,all} + P_{Batt} \quad (7)$$

$$P_{ME} \leq P_{ME,\,max} \quad (8)$$

$$P_{SG,min} \leq P_{SG} \leq 0 \wedge P_{SG} \leq -P_{PTO,limit} \quad (9)$$

$$P_{Gen,i} \leq 0.85 \times P_{Gen,max}\,, \forall\, i = 1,2,3 \quad (10)$$

$$SOC_{min} \leq SOC \leq SOC_{max} \quad (11)$$

Figure 3 illustrates the flowchart of the ECMS algorithm developed. This algorithm manages the operation of key components, including the ME, SG, gensets, battery, and propeller, by optimizing a cost function. The required input variables for the optimization are P_{Prop}, SOC, and $P_{Consumers}$.

The algorithm begins by defining a range for the control variables, based on the input data, mechanical and electrical balance conditions, and the physical constraints of the components. Next, it generates a cost function matrix that accounts for the dependencies on these control variables. The algorithm then identifies the optimal combination of P_{SG} and genset power values that minimizes the cost. This minimization process follows the approach outlined by Aletras et al. [29].

After completing the minimization process, eq. 6 and eq. 7 are used to define the values of P_{ME} and P_{Batt}. The parameters chosen for the ECMS algorithm are detailed in Table 2.

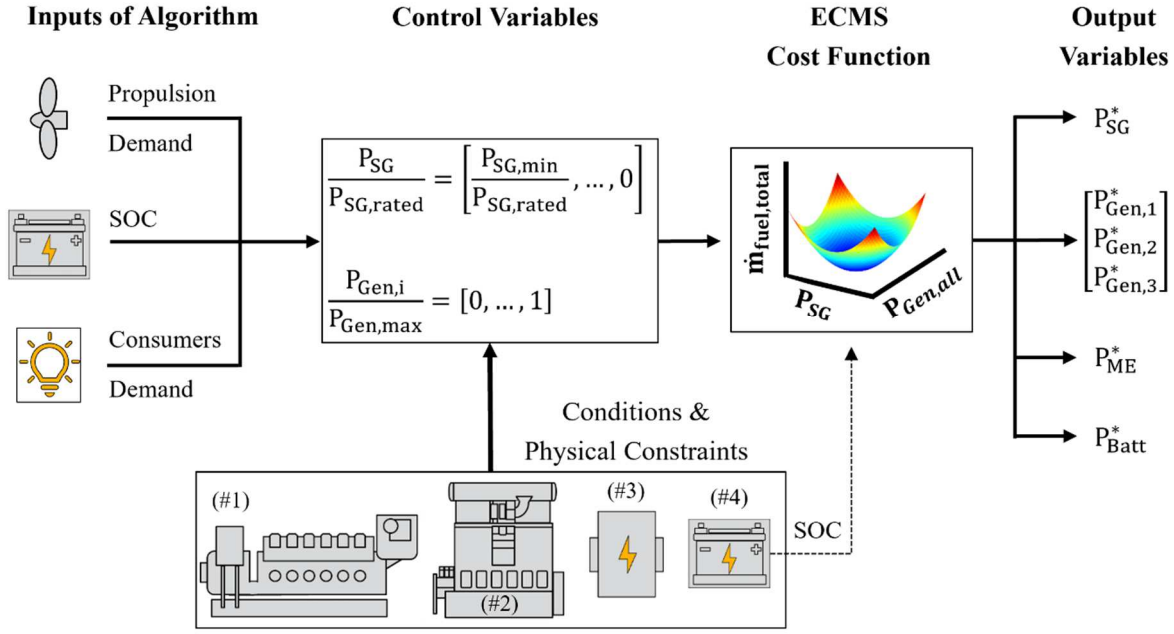

Figure 3. ECMS procedure overview. (#1): gensets, (#2): ME, (#3): shaft-generator (SG), (#4): battery pack, S_P: propeller position, P_{SG}: SG power, $P_{SG,rated}$: SG rated power, $P_{Gen,i}$: genset power for, $P_{Gen,max}$: maximum genset power, $P_{Gen,all}$: total power from all gensets, $P_{Gen,all}$: total power from all gensets, $\dot{m}_{fuel,total}$: ECMS cost function, P_{ME}: ME power, P_{Batt}: battery power

2.4 Examined operation phases

In the initial phase, FOC benefits of the ECMS are compared to those of a conventional configuration across different operation phases: port stay, open sea sailing, and port approach. To simulate these scenarios, real-world trip data, including propeller rotational speed and power demand from electrical consumers, are used from an anonymous deep-sea ship operating under similar conditions. Table 2 provides an overview of the profiles used for different operation phases. The activity durations are normalized relative to the open sea sailing phase, ensuring a common time frame across all scenarios. Additionally, the average speed and average electrical power demand are normalized to the main engine's rated speed and the rated power of a single genset, respectively. For the port stay phase, two distinct electrical demand scenarios are considered: one with cargo transfer operations ("Cargo On") and another without ("Cargo Off"). During the open sea sailing phase, two different electrical consumers power demand profiles are

analyzed: one with the ship's ventilation system activated ("Ventilation On") and one without it ("Ventilation Off"). For other phases, such as maneuvering or port approach, no specific electrical mode is applied, referred to as "Normal". Further details about the profiles can be found in [32], which also presents a hybrid engine room with a controllable pitch propeller.

Table 3. Operation phases and characteristics

Phase	Electrical Consumers Mode	Normalized Duration [-]	Average Normalized Speed [-]	Average Normalized Electrical Consumers Demand [-]
Port Stay	Cargo On	0.45	0	1.58
	Cargo Off	0.22	0	0.49
Open Sea Sailing (Design Speed: 22kn Max Speed:25kn [33])	Ventilation On	1	0.72	1.44
	Ventilation Off	1	0.72	0.91
From Port Maneuvering to Sailing	Normal	2.33	0.70	0.48
From Sailing to Port Maneuvering		2.33	0.14	0.42
6 kn port approach		0.3	0.17	1.39
12 kn port approach		0.3	0.22	1.39

2.5 FOC corrections

To ensure a fair comparison of any scenarios involving hybrid or conventional engine rooms, the energy supplied for propulsion and electrical consumers should be identical between the scenarios. Additionally, when a battery pack is used, comparisons should assume equal SOC levels at the beginning and end of the simulation. However, this condition is not always met. The use of dynamic simulators for engine room modeling can result in minor discrepancies in propeller and electrical power demands and may not consistently maintain SOC levels [13,15,34]. These issues could be mitigated by using a backward modeling simulator, which employs a quasi-static approach. However, this study utilizes a forward modeling simulator due to its basis in physical causality, which supports the development of online control strategies [31].

As shown in eq. 12, a correction method is proposed to ensure a fair comparison, adapting the approach of Aletras et al. [30] to the examined ship engine room. This is accomplished by normalizing the total simulated fuel consumption ($\mathrm{SE_{Fuel}}$) from the ME and gensets against the simulated energy demands at the propeller $\mathrm{SE_{Prop}}$ and electrical consumers ($\mathrm{SE_{Con}}$).

Comparing the normalized FOC energy with the total required energy allows for a fair comparison between engine room configurations. This approach is necessary because absolute FOC energy values can be misleading, as varying energy demands from the propeller and other consumers can affect the total FOC energy. The relative FOC reductions (FOCRs) are calculated by comparing the normalized corrected fuel energy consumption ($\widehat{\mathrm{CE}}_{\mathrm{Fuel}}$) values of the various configurations.

The new expression also incorporates a reference energy consumed from the battery ($\mathrm{RE_{Batt}}$) to ensure that the simulated battery energy consumption ($\mathrm{SE_{Batt}}$) is the same across the compared configurations. Since the conventional configuration lacks a battery, $\mathrm{RE_{Batt}}$ is set to zero. The efficiencies of the battery and gensets are assigned their average simulated values during the different phases ($\bar{\eta}_{\mathrm{Batt}}$ and $\bar{\eta}_{\mathrm{Gensets}}$, respectively).

$$\widehat{\mathrm{CE}}_{\mathrm{Fuel}} = \begin{cases} \left(\mathrm{A} + \mathrm{B} \times \left(\frac{1}{\bar{\eta}_{\mathrm{Batt}}}\right) \middle| \mathrm{SE_{Batt}} \geq \mathrm{RE_{Batt}}\right) \\ \left(\mathrm{A} + \mathrm{B} \times \bar{\eta}_{\mathrm{Batt}} | \mathrm{SE_{Batt}} < \mathrm{RE_{Batt}}\right) \end{cases} \quad (12)$$

$$\text{with: } \mathrm{A} = \frac{\mathrm{SE_{Fuel}}}{\mathrm{SE_{Prop}} + \mathrm{SE_{Con}}}, \mathrm{B} = \frac{(\mathrm{SE_{Batt}} - \mathrm{RE_{Batt}}) \times \left(\frac{1}{\bar{\eta}_{\mathrm{Gensets}}}\right)}{\mathrm{SE_{Prop}} + \mathrm{SE_{Con}}}$$

3 RESULTS

3.1 Port stay phase

Figure 4 shows the genset load profiles during a port stay event, where electricity is used to transfer cargo onto the ship ("port stay cargo on" – Table 3). The ME is off, so the hybrid configuration relies on both gensets and the battery to supply the energy needed by the electrical consumers. In contrast, the conventional configuration solely depends on the gensets to meet this demand.

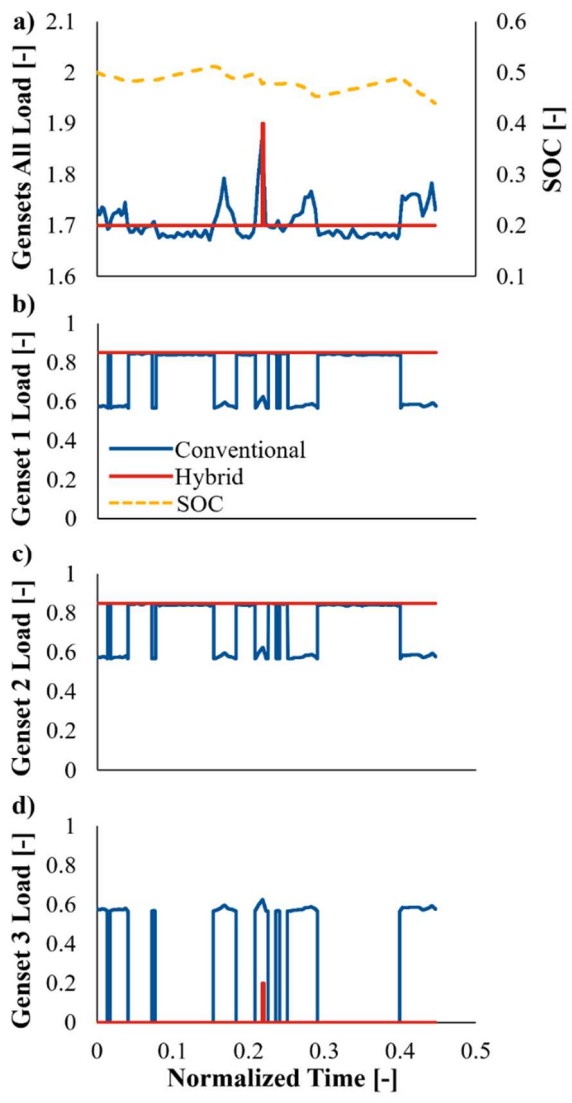

Figure 4. Gensets operation and SOC for the port stay cargo on with conventional and hybrid configurations. All gensets and SOC (a), genset 1 (b), genset 2 (c), genset 3 (d)

In the conventional configuration, the load on the gensets varies based on changes in power demand from electrical consumers and is distributed among the three gensets according to the rules shown in Figure 2. On the other hand, in the hybrid configuration, the gensets operate at a steady load, with genset #1 and genset #2 running at their maximum load capacity of 0.85. The battery functions as an energy buffer, compensating for the differences between the power supplied by the gensets and the power demanded by the electrical consumers, as shown in the SOC profile.

Between the normalized time interval of 0.20 and 0.25, a short surge occurs, necessitating the activation of the third genset. This happens due to an increase in power demand from the electrical consumers, while the ECMS algorithm works to keep the battery level stable at approximately 0.50.

Figure 5 illustrates the normalized net energy flows of the key components for both the conventional and hybrid configurations during the “port stay cargo on” phase. These energy flows are normalized relative to the energy demands of the electrical consumers. Since the ship remains stationary, only the electrical components of the configurations are considered. In the conventional configuration, the energy demand is distributed across all three gensets, while in the hybrid configuration, it is primarily met by gensets 1 and 2. Utilizing the ECMS algorithm, the hybrid configuration achieves a normalized FOC energy of 2.15, which is lower than the 2.22 observed in the conventional configuration. This reduction is due to the higher average efficiency of the gensets in the hybrid configuration, as they operate at a higher load compared to those in the conventional configuration, as depicted in Figure 4

Table 4 provides a summary of the FOCR and average genset efficiency ($\bar{\eta}_{\text{Gensets}}$) for both the port stay cargo on and cargo off phases. Alongside the cargo on scenario, the analysis includes the port stay cargo off phase, where the ship does not utilize electrical consumers for cargo operations while docked. The hybrid configuration achieves a 3.15% FOCR during the cargo on phase and 0.81% during the cargo off phase. The smaller benefit observed during the cargo off phase is due to a more modest improvement in genset efficiency.

Table 4. Gensets average efficiency and FOCR for the port stay cargo on and off

Phase	Configuration	Magnitude	
		$\bar{\eta}_{\text{Gensets}}$ [%]	FOCR [%]
Port Stay Cargo On	Conventional	45.0	--
	Hybrid	46.5	3.15
Port Stay Cargo Off	Conventional	42.9	--
	Hybrid	43.2	0.81

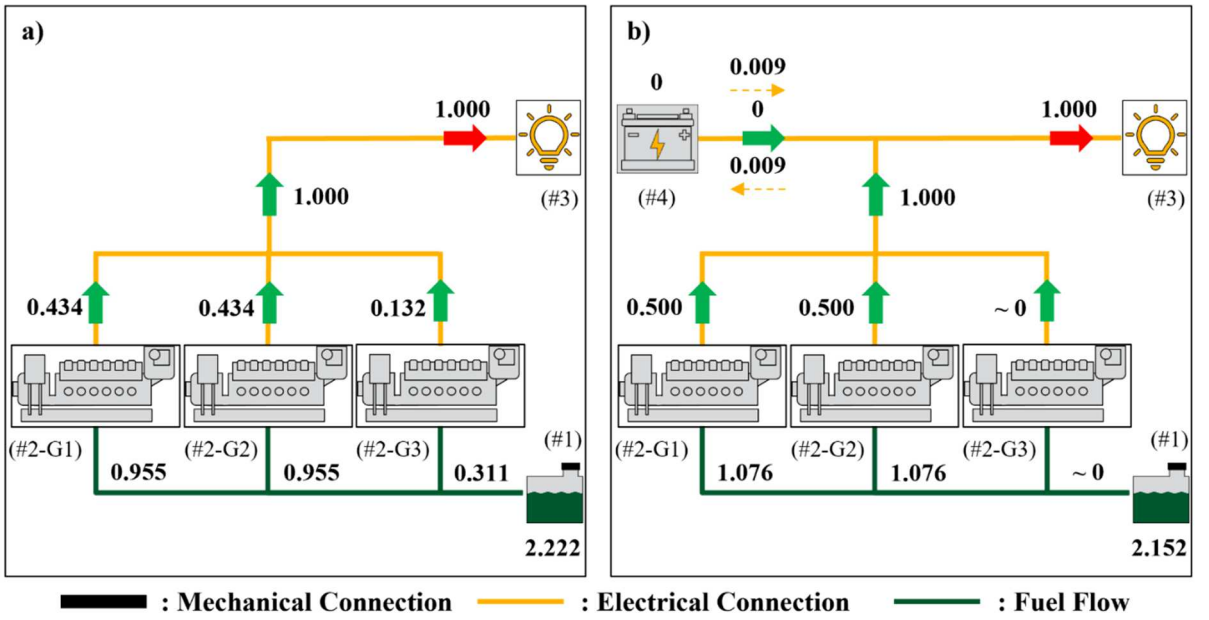

Figure 5. Energy flows analysis for port stay cargo on for the conventional (a) and the hybrid (b) configurations, where (#1): fuel tank, (#2): ME, (#3): propeller, (#4-G1): genset 1, (#4-G2): genset 2, (#4-G3): genset 3, (#5): electrical consumers, (#6): SG, (#7): battery pack

3.2 Open sea sailing phase

Figure 6 illustrates the operating points of the ME during open sea sailing with the ship's ventilation system turned off, a condition referred to as "open sea sailing ventilation off" (Table 2). In the conventional configuration, the ME load follows the propeller resistance curve to propel the ship, while the gensets handle all electrical loads. In contrast, the hybrid configuration has the ME operating at a higher load, supplying power not only to the propeller but also to the SG for electricity production. This arrangement fully meets the demands of the electrical consumers, leaving the gensets inactive, as detailed in Table 5.

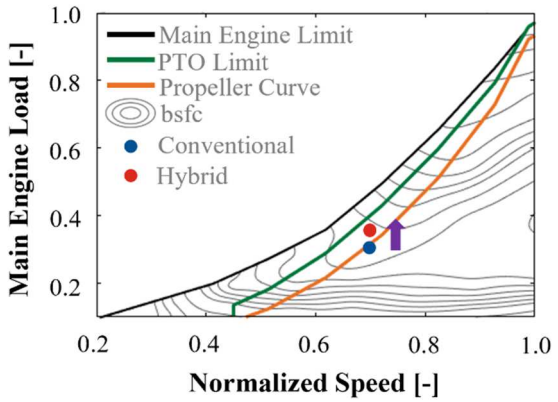

Figure 6. Operating power for ME in open sea sailing ventilation off

Table 5. Gensets load for open sea sailing ventilation off in conventional and hybrid configurations

Configuration	Operating load [-] per Genset			
	All Gensets	Genset 1	Genset 2	Genset 3
Conventional	0.90	0.45	0.45	0.00
Hybrid	0.00	0.00	0.00	0.00

Figure 7 depicts the normalized net energy flows during open-sea sailing with ventilation turned off. In the hybrid configuration, the ME uses more fuel oil than in the conventional configuration because it supplies both propulsion and electrical power. However, the total normalized fuel consumption, accounting for both the ME and the gensets, is 1.77 in the hybrid configuration, compared to 1.89 in the conventional one. This difference is primarily due to the greater efficiency of the two-stroke ME at high loads compared to the four-stroke gensets.

Table 6 summarizes the average efficiencies of the ME ($\bar{\eta}_{ME}$), SG ($\bar{\eta}_{SG}$), $\bar{\eta}_{Gensets}$, and the FOCR for open sea sailing under two scenarios: ventilation off and on. The hybrid configuration achieved overall FOCRs of 6.3% and 3.2% with ventilation off and on, respectively.

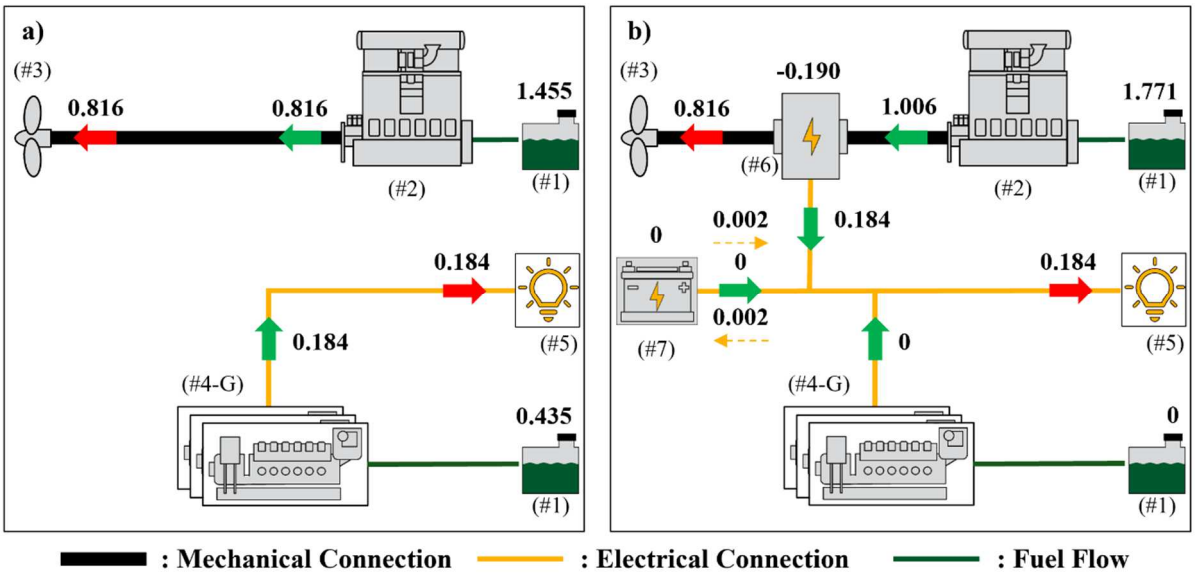

Figure 7. Energy flows for open sea sailing ventilation off in conventional (a) and hybrid (b) configurations, where (#1): fuel tank, (#2): ME, (#3): propeller, (#4-G): gensets, (#5): electrical consumers, (#6): shaft-generator, (#7): battery pack

In the hybrid configuration, the PTO mode is activated, allowing the ME to operate at high load, thereby improving efficiency. Additionally, the ME paired with the SG produces electrical power more efficiently than the gensets. However, when ventilation is on, the SG alone cannot meet the power demand, requiring the gensets to supplement, which slightly reduces the FOC benefits of the hybrid system compared to the ventilation-off scenario.

Table 6. Component energy efficiencies and FOCR during open sea sailing with two ventilation scenarios

Ventilation	Configuration	Magnitude			
		$\bar{\eta}_{ME}$ [%]	$\bar{\eta}_{SG}$ [%]	$\bar{\eta}_{Gensets}$ [%]	FOCR [%]
Off	Conventional	56.1	--	42.3	--
	Hybrid	56.8	96.8	--	-6.30
On	Conventional	56.1	--	46.0	--
	Hybrid	56.6	96.9	46.6	-3.18

3.3 Port entering and leaving modes

Figure 8 illustrates the operational performance as the ship approaches the port at 6 kn, comparing the normalized shaft speed, loads of the SG, ME, and gensets, as well as the SOC between conventional and hybrid configurations. The shaft speed is expressed as a ratio of the ME's rated speed, and the model accurately tracks the target rotational speed. During normalized time intervals from 0 to 0.06, the ECMS algorithm choses SG operation, causing the ME in the hybrid configuration to run at a higher load compared to the conventional configuration to power both the propeller and the SG. Consequently, gensets contribute less power in hybrid configuration (Figure 8d) but remain active to some extent.

During the normalized time interval from 0.06 to 0.12, the rotational speed decreases, leading the ECMS to deactivate PTO operation in the hybrid configuration due to the ME's physical limitations. As a result, the SG is turned off, and the ME load decreases to match the levels seen in the conventional configuration. With the SG inactive, the ECMS activates the gensets to supply electrical power and maintain the battery SOC within the desired range.

During the 0.12 to 0.30 interval, the ME is turned off in all configurations as the ship reaches a complete stop. In the conventional configuration, gensets exclusively supply the electrical power, whereas in the hybrid configuration, the demand is met using a combination of the gensets and batteries.

Table 7 provides a summary of component efficiencies and FOCR during the 6 kn approach. In the hybrid configuration, the higher ME load driven by PTO operation results in improved efficiency compared to the conventional configuration. Furthermore, the hybrid configuration operates gensets at higher loads, further enhancing their efficiency relative to the conventional configuration.

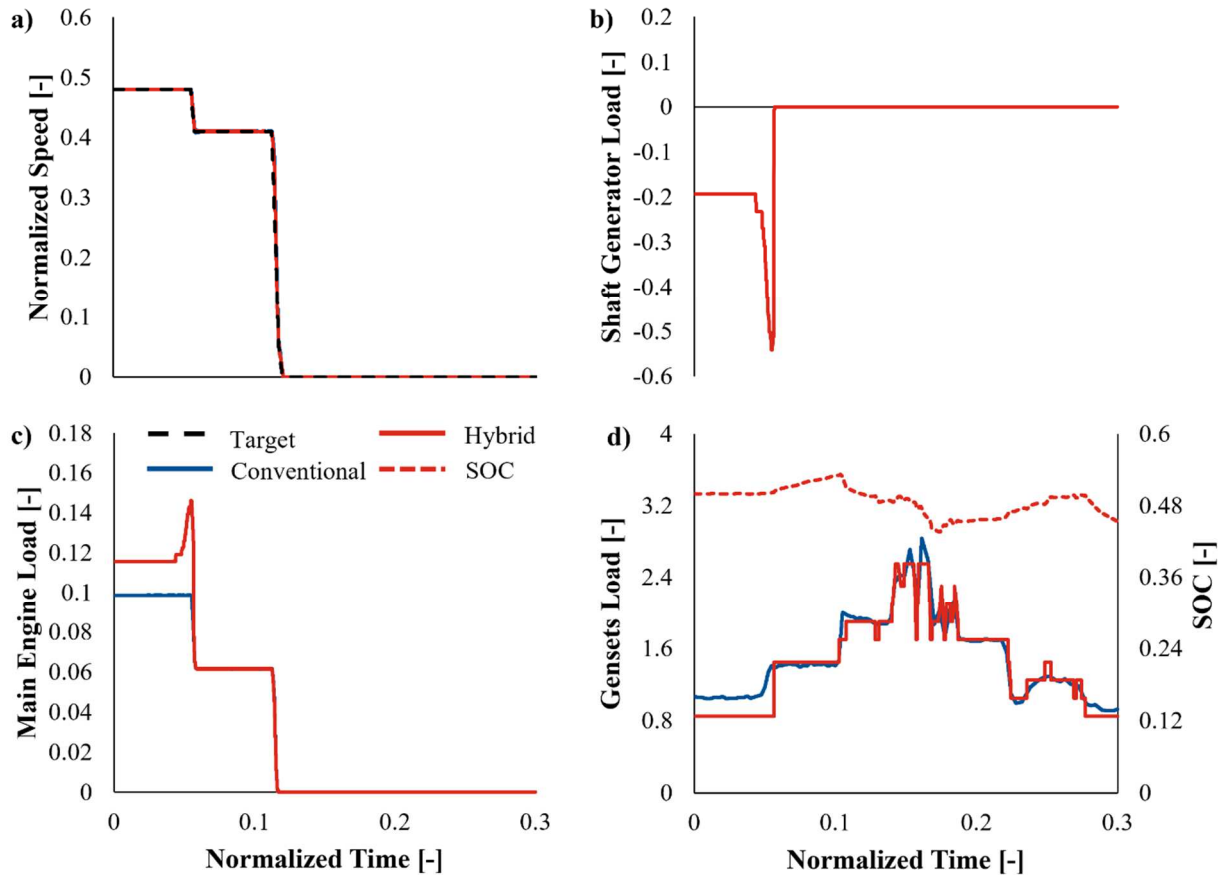

Figure 8. Engine room operation during port approach 1, propeller rotational speed (a), SG load (b), ME load (c), gensets load (d)

Table 7. Component energy efficiencies and FOCR during port approach at 6 kn

Configuration	Magnitude			
	$\bar{\eta}_{ME}$ [%]	$\bar{\eta}_{SG}$ [%]	$\bar{\eta}_{Gensets}$ [%]	FOCR [%]
Conventional	42.9	--	44.4	--
Hybrid	43.9	92.3	45.4	-1.94

As in previous cases, another factor contributing to improved FOC is the higher efficiency of electricity generation by the ME+SG compared to the gensets. Overall, the hybrid configuration achieves a 1.94% FOC improvement over the conventional configuration. For other phases, including in-port and port approach operations, the hybrid configuration offers FOC benefits ranging from 2.40% to 3.6% (Table 8).

Table 8. Summary of benefits for different operation phases offered by hybrid over conventional configuration

Phase	FOCR from Hybrid over Conventional [%]
From port maneuvering to sailing	2.40
From sailing to port maneuvering	2.87
6 kn approach	1.94
12 kn approach	3.60

4 DISCUSSION AND CONCLUSIONS

This study investigates how the fuel oil consumption of a two-stroke engine deep-sea ship can be reduced by integrating a shaft generator and batteries into a hybrid propulsion system. To facilitate this, a novel adaptive ECMS algorithm was developed using real operational data. The hybrid propulsion system, combined with ECMS control, achieved efficiency improvements of up to 6.0%, varying with the ship's operating phase, with the most significant gains observed during open

sea sailing. These benefits largely result from the higher efficiency of the ME operating at increased loads in PTO hybrid mode and the more efficient electricity generation by the SG compared to the gensets in the conventional configuration. This efficiency advantage stems from the higher thermal efficiency of the ME's two-stroke combustion relative to the gensets' four-stroke combustion. However, the fuel savings are less pronounced during port stay phases where PTO operation is not feasible.

The range of consumption improvements observed in this study can be compared to the 11% improvement reported by Kim et al. [35] and the 1.6–18.9% savings noted by Diniz et al. [36]. Both studies used ECMS for hybrid control and demonstrated advantages over conventional operation in fishing boats (Kim et al. [35]) and shuttle tankers and tugboats (Diniz et al. [36]). However, unlike the present study, these works did not focus on deep-sea ships. Other published results using different EMS algorithms include the study by Al-Falahi et al. [37], which showed that a rule-based algorithm achieved a 2.9% benefit from hybrid operation, while a grey-wolf optimization strategy increased this to 7.5%. Additionally, Planakis et al. [38] proposed a nonlinear model MPC approach for hybrid control, yielding a 2% improvement.

While the efficiency gains may seem modest, they remain significant when considering that retrofitting a SG and a battery pack is one of the simplest upgrades a ship can undertake to meet CII and EEXI compliance. These technologies are also readily applicable to new builds. Furthermore, another alternative being examined nowadays is reducing the vessel's cruising speed to lower CO_2 emissions. However, by leveraging the CO_2 benefits of hybridization, such a sacrifice is not necessary. Further to hybridization, enhanced ECMS control algorithms can further optimize efficiency, highlighting the need to move beyond traditional rule-based approaches. In a commercial EMS implementation, additional functionalities, such as managing auxiliary systems and emission control devices like scrubbers and SCR, should be incorporated. The specific benefits will vary depending on the ship type and operational conditions but can be accurately calculated once real-world operational profiles are available. A key advantage of ECMS is their adaptability to various applications without sacrificing general applicability, unlike rule-based approaches, which require extensive fine-tuning for each specific use case.

5 DEFINITIONS, ACRONYMS, ABBREVIATIONS

AC	Alternating current
BSFOC	Brake specific fuel oil consumption
CII	Carbon intensity indicator
CO2	Carbon dioxide
DC	Direct current
DP	Dynamic programming
ECMS	Equivalent minimization consumption strategy
EEDI	Energy efficiency design index
EEXI	Energy efficiency existing ship index
EMS	Energy management system
FOC	Fuel oil consumption
FOCR	FOC reduction
IMO	International maritime organization
ME	Main engine
MPC	Model predictive control
PTO	Power take-off operation
SG	Shaft-generator
SOC	State of charge
$\overline{\eta}_{ME}$	Average ME efficiency
$\overline{\eta}_{Gensets}$	Average gensets efficiency
$\overline{\eta}_{SG}$	Average SG efficiency

6 ACKNOWLEDGMENTS

The authors would like to acknowledge support of this work by the personnel of the WinGD team for providing the data of the powertrain. The research work was supported by the Hellenic Foundation for Research and Innovation (HFRI) under the HFRI PhD Fellowship grant (Fellowship Numbers: 6653).

7 DECLARATION OF GENERATIVE AI AND AI-ASSISTED TECHNOLOGIES IN THE WRITING PROCESS

During the preparation of this work the authors used Gemini and ChatGPT in order to improve language and readability, with caution. After using this tool/service, the authors reviewed and edited the content as needed and take full responsibility for the content of the publication.

8 REFERENCES AND BIBLIOGRAPHY

1. Hansen, J.E., Sato, M., Simons, L., Nazarenko, L.S., Sangha, I., Kharecha, P., Zachos, J.C., Schuckmann, K. von, Loeb, N.G., Osman, M.B., Jin, Q., Tselioudis, G., Jeong, E., Lacis, A., Ruedy, R., Russell, G., Cao, J., and Li, J., "Global warming in the pipeline," *Oxford Open Clim. Chang.* 3(1), 2023, doi:10.1093/oxfclm/kgad008.

2. IEA, "CO2 Emissions in 2022," https://www.iea.org/reports/co2-emissions-in-2022, Mar. 2024.

3. Cars, planes, trains: where do CO2 emissions from transport come from?, https://ourworldindata.org/co2-emissions-from-transport.

4. IMO, "2023 IMO Strategy on Reduction of GHG Emissions from Ships," https://www.imo.org/en/OurWork/Environment/Pages/2023-IMO-Strategy-on-Reduction-of-GHG-Emissions-from-Ships.aspx, Mar. 2024.

5. IMO, "IMO's work to cut GHG emissions from ships," https://www.imo.org/en/MediaCentre/HotTopics/Pages/Cutting-GHG-emissions.aspx, Mar. 2024.

6. DNV, "CII – Carbon Intensity Indicator," https://www.dnv.com/maritime/insights/topics/CII-carbon-intensity-indicator/answers-to-frequent-questions.html, Mar. 2024.

7. IMO, "Improving the energy efficiency of ships," https://www.imo.org/en/OurWork/Environment/Pages/Improving the energy efficiency of ships.aspx, Mar. 2024.

8. Inal, O.B., Charpentier, J.-F., and Deniz, C., "Hybrid power and propulsion systems for ships: Current status and future challenges," *Renew. Sustain. Energy Rev.* 156:111965, 2022, doi:10.1016/j.rser.2021.111965.

9. Geertsma, R.D., Negenborn, R.R., Visser, K., and Hopman, J.J., "Design and control of hybrid power and propulsion systems for smart ships: A review of developments," *Appl. Energy* 194:30–54, 2017, doi:10.1016/j.apenergy.2017.02.060.

10. Fan, A., Li, Y., Liu, H., Yang, L., Tian, Z., Li, Y., and Vladimir, N., "Development trend and hotspot analysis of ship energy management," *J. Clean. Prod.* 389:135899, 2023, doi:10.1016/j.jclepro.2023.135899.

11. Roslan, S.B., Konovessis, D., and Tay, Z.Y., "Sustainable Hybrid Marine Power Systems for Power Management Optimisation: A Review," *Energies* 15(24):9622, 2022, doi:10.3390/en15249622.

12. Zhang, Y., Xue, Q., Gao, D., Shi, W., and Yu, W., "Two-level model predictive control energy management strategy for hybrid power ships with hybrid energy storage system," *J. Energy Storage* 52:104763, 2022, doi:10.1016/j.est.2022.104763.

13. Planakis, N., Papalambrou, G., and Kyrtatos, N., "Ship energy management system development and experimental evaluation utilizing marine loading cycles based on machine learning techniques," *Appl. Energy* 307:118085, 2022, doi:10.1016/j.apenergy.2021.118085.

14. Antonopoulos, S., Visser, K., Kalikatzarakis, M., and Reppa, V., "MPC Framework for the Energy Management of Hybrid Ships with an Energy Storage System," *J. Mar. Sci. Eng.* 9(9):993, 2021, doi:10.3390/jmse9090993.

15. Chua Wan Yuan, L., Tjahjowidodo, T., Lee, G.S.G., and Chan, R., "Optimizing fuel savings and power system reliability for all-electric hybrid vessels using Model Predictive Control," *2017 IEEE International Conference on Advanced Intelligent Mechatronics (AIM)*, IEEE, ISBN 978-1-5090-5998-0: 1532–1537, 2017,

doi:10.1109/AIM.2017.8014236.

16. Xie, P., Guerrero, J.M., Tan, S., Bazmohammadi, N., Vasquez, J.C., Mehrzadi, M., and Al-Turki, Y., "Optimization-Based Power and Energy Management System in Shipboard Microgrid: A Review," *IEEE Syst. J.* 16(1):578–590, 2022, doi:10.1109/JSYST.2020.3047673.

17. Chua, L.W.Y., Tjahjowidodo, T., Seet, G.G.L., and Chan, R., "Implementation of Optimization-Based Power Management for All-Electric Hybrid Vessels," *IEEE Access* 6:74339–74354, 2018, doi:10.1109/ACCESS.2018.2883324.

18. Liza Chua Wan Yuan, Tjahjowidodo, T., Gerald Seet Gim Lee, Chan, R., and Adnanes, A.K., "Equivalent Consumption Minimization Strategy for hybrid all-electric tugboats to optimize fuel savings," *2016 American Control Conference (ACC)*, IEEE, ISBN 978-1-4673-8682-1: 6803–6808, 2016, doi:10.1109/ACC.2016.7526743.

19. Zhu, J., Chen, L., Wang, X., and Yu, L., "Bi-level optimal sizing and energy management of hybrid electric propulsion systems," *Appl. Energy* 260:114134, 2020, doi:10.1016/j.apenergy.2019.114134.

20. Kalikatzarakis, M., Geertsma, R.D., Boonen, E.J., Visser, K., and Negenborn, R.R., "Ship energy management for hybrid propulsion and power supply with shore charging," *Control Eng. Pract.* 76:133–154, 2018, doi:10.1016/j.conengprac.2018.04.009.

21. Chua, L.W.Y., "A strategy for power management of electric hybrid marine power systems," Nanyang Technological University, 2019, doi:10.32657/10220/48078.

22. Dedes, E.K., Hudson, D.A., and Turnock, S.R., "Investigation of Diesel Hybrid systems for fuel oil reduction in slow speed ocean going ships," *Energy* 114:444–456, 2016, doi:10.1016/j.energy.2016.07.121.

23. Sui, C., Stapersma, D., Visser, K., Vos, P. de, and Ding, Y., "Energy effectiveness of ocean-going cargo ship under various operating conditions," *Ocean Eng.* 190:106473, 2019, doi:10.1016/j.oceaneng.2019.106473.

24. MathWorks, "Simulink," https://www.mathworks.com/products/simulink.html, Mar. 2024.

25. MathWorks, "Powertrain Blockset," https://www.mathworks.com/products/powertrain.html, Mar. 2024.

26. WinGD, "X-EL - Energy Management," https://www.wingd.com/en/technology-innovation/hybrid-energy-systems/, Mar. 2024.

27. WinGD, "X62DF-2.1," https://www.wingd.com/en/engines/engine-types/x-df-dual-fuel/x62df-2-1/, Mar. 2024.

28. HD Hyundai Heavy Industries, "Hi-touch Marine & Stationary ENgine," https://www.hyundai-engine.com/en/aboutus/Himsen, Mar. 2024.

29. Aletras, N., Doulgeris, S., Samaras, Z., and Ntziachristos, L., "Comparative Assessment of Supervisory Control Algorithms for a Plug-In Hybrid Electric Vehicle," *Energies* 16(3):1497, 2023, doi:10.3390/en16031497.

30. Aletras, N., Broekaert, S., Bitsanis, E., Fontaras, G., Samaras, Z., and Ntziachristos, L., "Energy management algorithm based on average power demand prediction for plug-in hybrid electric trucks," *Energy Convers. Manag.* 299:117785, 2024, doi:10.1016/j.enconman.2023.117785.

31. Onori, S., Serrao, L., and Rizzoni, G., "Hybrid Electric Vehicles," Springer London, London, ISBN 978-1-4471-6779-2, 2016, doi:10.1007/978-1-4471-6781-5.

32. Aletras, N., Karvountzis-Kontakiotis, A., Kefalas, N., Grigoriadis, A., Samaras, Z., and Ntziachristos, L., "Optimization-Based Energy Management Algorithm for 2-Stroke Hybrid Ship with Controllable Pitch Propeller," *J. Mar. Sci. Eng.* 12(12):2331, 2024, doi:10.3390/jmse12122331.

33. RO/RO ships : TØNSBERG, https://www.mhi.com/products/ship/roro_tonsberg.html, Dec. 1BC.

34. Chan, R.R., Chua, L., and Tjahjowidodo, T., "Enabling technologies for sustainable all — Electric hybrid vessels (Invited paper)," *2016 IEEE International Conference on*

Sustainable Energy Technologies (ICSET), IEEE, ISBN 978-1-5090-5200-4: 401–406, 2016, doi:10.1109/ICSET.2016.7811818.

35. Kim, S., Jeon, H., Park, C., and Kim, J., “Lifecycle Environmental Benefits with a Hybrid Electric Propulsion System Using a Control Algorithm for Fishing Boats in Korea,” *J. Mar. Sci. Eng.* 10(9):1202, 2022, doi:10.3390/jmse10091202.

36. Diniz, G.H.S., Miranda, V. dos S., and Carmo, B.S., “Dynamic modelling, simulation, and control of hybrid power systems for escort tugs and shuttle tankers,” *J. Energy Storage* 72:108091, 2023, doi:10.1016/j.est.2023.108091.

37. Al-Falahi, M.D.A., Nimma, K.S., Jayasinghe, S.D.G., Enshaei, H., and Guerrero, J.M., “Power management optimization of hybrid power systems in electric ferries,” *Energy Convers. Manag.* 172:50–66, 2018, doi:10.1016/j.enconman.2018.07.012.

38. Planakis, N., Papalambrou, G., and Kyrtatos, N., “Predictive power-split system of hybrid ship propulsion for energy management and emissions reduction,” *Control Eng. Pract.* 111:104795, 2021, doi:10.1016/j.conengprac.2021.104795.

9 CONTACT

Prof. Leonidas Ntziachristos

Tel.: +30 2310 996003

E-mail address: leon@auth.gr

10 APPENDIX A

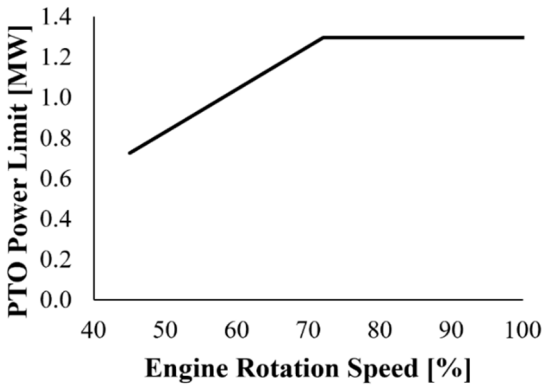

Figure A 1. PTO power limit for the SG operating power